atoms

MDPI

Article

Few Body Effects in the Electron and Positron Impact Ionization of Atoms

R.I. Campeanu [1,*] and Colm T. Whelan [2]

[1] Department of Physics and Astronomy, York University, Toronto, ON M3J 1P3, Canada
[2] Physics Department, Old Dominion University, Norfolk, VA 23529, USA; cwhelan@odu.edu
* Correspondence: campeanu@yorku.ca

Abstract: Triple differential cross sections (TDCS) are presented for the electron and positron impact ionization of inert gas atoms in a range of energy sharing geometries where a number of significant few body effects compete to define the shape of the TDCS. Using both positrons and electrons as projectiles has opened up the possibility of performing complementary studies which could effectively isolate competing interactions that cannot be separately detected in an experiment with a single projectile. Results will be presented in kinematics where the electron impact ionization appears to be well understood and using the same kinematics positron cross sections will be presented. The kinematics are then varied in order to focus on the role of distortion, post collision interaction (pci), and interference effects.

Keywords: ionization; electron; positron; few body

Citation: Campeanu, R.I.; Whelan, C.T. Few Body Effects in the Electron and Positron Impact Ionization of Atoms. *Atoms* **2021**, *9*, 33. https://doi.org/10.3390/atoms9020033

Academic Editor: Grzegorz Piotr Karwasz

Received: 4 May 2021
Accepted: 1 June 2021
Published: 9 June 2021

1. Introduction

In a coincidence experiment, a projectile of momentum k_0, energy E_0 impinges on a target atom and ionizes it. The ejected electron and scattered projectile are detected with their angles and energies resolved. The momentum vectors of the scattered projectile, k_1 and the ejected electron, k_2, form a plane and thus we can define all possible kinematics by the set $(k_0, k_1, k_2, \Phi, \theta_1, \theta_2)$, where Φ defines the angle k_0 makes to the plane of detection, the "gun angle", see Figure 1.

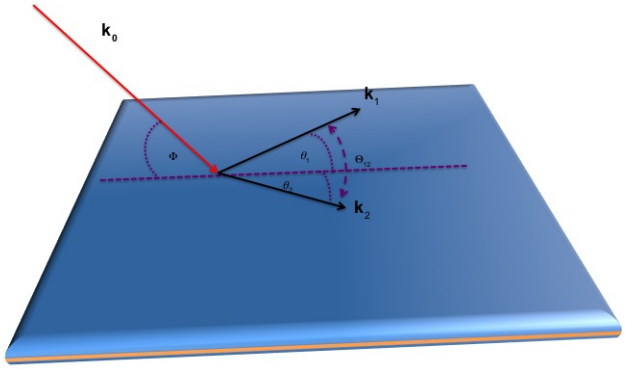

Figure 1. The incoming projectile has momentum $\mathbf{k}_0$ and energy E_0, and it comes in at an angle Φ with respect to the plane in which the two final state particles are detected at angles θ_1, θ_2 with respect to the projection of the incoming direction on their plane. $\Phi = 0^\circ$ corresponds to coplanar geometry, $\Phi = 90^\circ$ to perpendicular plane geometry. Θ_{12} is the angle between the two detected particles.

The great advantage of the coincidence approach is that it allows us to focus on particular geometries and kinematics where three subtle body effects can be observed. In less differential measurements, these effects will be swamped by the gross features of the interactions. Thus far, complementary studies of electron and positron impact

ionization have been restricted to asymmetric geometries [1–3] with $E_1 >> E_2$, and θ_1 small where the triple differential cross section tends to have the same character as the first Born approximation, being symmetric about the direction of momentum transfer with the only significant structures coming from target wave function effects [4]. In these kinematics, it is particularly difficult to disentangle the different few body contributions [5,6]; this problem is enhanced because what few differences there are tend to be in the absolute size of the cross section which is extremely demanding to measure accurately [7]. In this paper, we focus on energy sharing geometries and explore the possibility of observing differences in the shape of the cross section. In energy sharing geometries, we are dealing with a "hard collision" where the incident electron loses more than half its energy; conservation of momentum then requires the lost projectile momentum to be carried off by the recoiling ion and we would, therefore, expect the nucleus to play an important role. The conventional second Born approximation struggles to include the $e^{\pm}$ interaction with the nucleus [8] and is not best suited for these geometries. A full close coupling calculation would be ideal that is very computationally demanding, and it is not readily applicable to multi-electron targets [5,9,10]. Our ambition here is to focus on mechanisms and to give direction to the ongoing coincidence studies of electron and positron impact ionization. The distorted wave Born approximation (DWBA) [11–13] is only the first order in the projectile—target electron interaction; however, it allows for the elastic scattering of the incoming projectiles and outgoing particles in the field of the atom/ion. Furthermore, the DWBA has provided excellent agreement with electron impact ionization in energy sharing kinematics and, because of its relative simplicity and flexibility, is an ideal vehicle to explore positron scattering and the different few body mechanisms.

2. Scattering Approximations

2.1. Electron Impact

In the DWBA, the TDCS for ionization of the nl orbital of an inert gas atom is given by:

$$\frac{d^3\sigma}{d\Omega_1 d\Omega_2 dE} = 2(2\pi)^4 \frac{k_1 k_2}{k_0} \sum_{m=-l}^{l} [|f_{nlm}|^2 + |g_{nlm}|^2 - Re(f^*_{nlm} g_{nlm})] \quad (1)$$

where f is the direct amplitude and g the exchange amplitude. In the DWBA, the direct and exchange amplitudes are given by

$$\begin{aligned} f_{nlm}(\mathbf{k}_1, \mathbf{k}_2) &= \langle \chi^-(\mathbf{k}_1, \mathbf{r}_1) \chi^-(\mathbf{k}_2, \mathbf{r}_2) | \tfrac{1}{\|\mathbf{r}_1 - \mathbf{r}_2\|} | \chi_0^+(\mathbf{k}_0, \mathbf{r}_1) \psi_{nlm}(\mathbf{r}_2) \rangle \\ g_{nlm}(\mathbf{k}_1, \mathbf{k}_2) &= \langle \chi^-(\mathbf{k}_1, \mathbf{r}_2) \chi^-(\mathbf{k}_2, \mathbf{r}_1) | \tfrac{1}{\|\mathbf{r}_1 - \mathbf{r}_2\|} | \chi_0^+(\mathbf{k}_0, \mathbf{r}_1) \psi_{nlm}(\mathbf{r}_2) \rangle \end{aligned} \quad (2)$$

In (2), $\chi_0^+(\mathbf{k}_0, \mathbf{r}_1)$ is the distorted-wave representing the incident electron and is calculated in the static-exchange potential of the neutral atom. The χ^-'s are the distorted waves that are calculated in the static-exchange potentials of the ion and then orthogonalized to ψ_{nlm}. These are normalized to a delta function i.e.,

$$\langle \chi^{\pm}(\mathbf{k}, \mathbf{r}) | \chi^{\pm}(\mathbf{k}', \mathbf{r}) \rangle = \delta(\mathbf{k} - \mathbf{k}') \quad (3)$$

For the target wave functions, we use the Hartree–Fock orbitals given in [14]. The electron–electron interaction occurs exactly once, and no account is taken of post collisional interaction (pci) between the two final state electrons. In our calculations below, the full non-local exchange potential is not used and rather a localized version [13,15–18] is employed. Its use greatly simplifies the static exchange calculations in that one only needs to solve differential rather than integro-differential equations. Because we treat each of the exiting electrons as moving in the field of a spin $\frac{1}{2}$ ion, there is an inherent ambiguity in the choice of exchange potential in the final channels, and we could choose it to be singlet or triplet [9,13]. For most energies, there is little or no difference between results calculated with the singlet or triplet potentials [13,18], but, at low energies, there is a weakness in the singlet form in that, for some energies, it can become complex. A method has been

proposed in [16] to make the potential real again if this happens, but this method results in a discontinuous singlet potential and generally gives results in poorer agreement with experiments than the equivalent triplet calculation, see [4,13]. In addition, we orthogonalize both outgoing waves to the bound orbital ψ_{nlm} so that the direct amplitude f_{nlm} has the correct behavior as the momentum transfer $\mathbf{q} \equiv \mathbf{k}_0 - \mathbf{k}_1$ tends to zero.

We can explore the effect of elastic scattering by the atom/ion by "switching" these interactions on and off in (2). This can lead to some interesting insights into what is happening and is a way of investigating multiple scattering mechanisms [12,19]. For example, by replacing the distorted wave $\chi_0^+(\mathbf{k}_0, \mathbf{r}_1)$ with a plane wave $(2\pi)^{-3/2} e^{i\mathbf{k}_0}$, we effectively "switch-off" the interaction between the incoming projectile and the atom.

The neglect of pci will be important at low energies [12,20]. To take some account of it, a Gamow factor N_{e-e-} [12,21] has been employed:

$$\frac{d^3\sigma^{DWBApci}}{d\Omega_1 d\Omega_2 dE} = N_{e-e-} \frac{d^3\sigma^{DWBA}}{d\Omega_1 d\Omega_2 dE} \tag{4}$$

where

$$N_{e-e-} = \frac{\gamma}{e^\gamma - 1} \tag{5}$$

with

$$\gamma = \frac{2\pi}{\|\mathbf{k}_1 - \mathbf{k}_2\|} \tag{6}$$

The N_{e-e-} factor tends to give the dominant angular behavior of the TDCS at low energies, and it does correctly force the cross section to go to zero when $\mathbf{k}_1 = \mathbf{k}_2$. However, the overall normalization is lost. To ameliorate this, it is has been proposed [4,17] to normalize N_{e-e-} so that it is fixed to 1 when the angle between $\mathbf{k}_1$ and $\mathbf{k}_2$ is 180°, i.e., when we have a colinear arrangement. A modified version of the N_{e-e-} factor has been suggested by Ward and Macek [22]. These authors suggested replacing N_{e-e-} with

$$M_{e-e-} = N_{e-e-} |{}_1F_1(-i\nu_3, 1, -2ik_3 r_{3av})|^2 \tag{7}$$

where

$$\begin{aligned} k_3 &= \tfrac{1}{2}\|\mathbf{k_1} - \mathbf{k_2}\| \\ \nu_3 &= -\tfrac{1}{\|\mathbf{k_1} - \mathbf{k_2}\|} \\ r_{3av} &= \tfrac{3}{\epsilon}[\tfrac{\pi}{4\sqrt{(3)}}(1 + \tfrac{0.627}{\pi}\sqrt{\epsilon}\ln\epsilon)]^2 \end{aligned} \tag{8}$$

with ϵ being the total energy of the two emerging electrons. The factor r_{3av} was chosen by the requirement that the M_{e-e-} factor reproduces the correct Wannier threshold law. In this way, it is hoped that M_{e-e-} should be able to stand on its own without renormalization. Certainly at low energies, this hope was not realized in the case of helium or hydrogen [4].

2.2. Positron Scattering

The DWBA TDCS equations look similar to (1) and (2), except that, in this case, there is no exchange amplitude g_{nlm} and the distorted-waves $\chi_0^+(\mathbf{k}_0, \mathbf{r}_1)$ and $\chi^-(\mathbf{k}_1, \mathbf{r}_1)$ for the positron are generated in the static potential, which is the minus of the static potential for electron impact. The distorted-wave $\chi^-(\mathbf{k}_2, \mathbf{r}_2)$ for the slow ejected electron is orthogonalized to the bound state. There is now no longer any ambiguity in the choice of exchange potential. The ground state of our targets is spin singlet ($S = 0$) and therefore the ejected electron wave function must be calculated in the singlet static-exchange potential.

To estimate pci, we now change the sign of γ in (5).

$$N_{e+e-} = \frac{\Gamma}{e^\Gamma - 1} \tag{9}$$

with

$$\Gamma = -\frac{2\pi}{\|\mathbf{k}_1 - \mathbf{k}_2\|} \tag{10}$$

We still have the problem of choosing a normalization. Once again, we could assume that, when the three particles are colinear ($\theta_{12} = 180^\circ$), the pci effects are minimal and normalize $N_{e^+e^-} = 1$ at the point. This is not ideal but is probably the best we can do. An undesirable feature is that, while $N_{e^-e^-} \to 0$ as $\Theta_{12} \to 0$, $N_{e^+e^-}$ goes to infinity in this limit, see Figure 2.

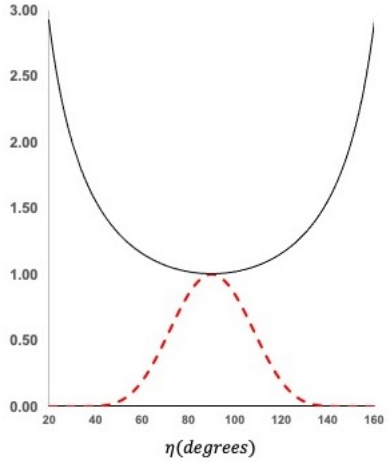

Figure 2. Plot of the Gamov factors for electron, dashed red and positron, solid black, with $\theta_1 = \theta_2, E_1 = E_2 = 1$ eV.

3. Results

3.1. Coplanar Symmetric Geometry

In these geometries, both outgoing particles have equal energies $E_1 = E_2$ and are detected with the same angle,

$$\eta = \theta_1 = \theta_2 = \frac{\Theta_{12}}{2} \tag{11}$$

The incoming projectile loses more than half its kinetic energy in the interaction; in such a "hard" collision, one expects collisions with the nucleus to play an important role and, as such, they are ideal testing grounds for the DWBA. There are a number of interesting experiments in coplanar symmetric geometry (i.e., $\Phi = 0^\circ$) [23–25]. For impact energies between 500 eV and 100 eV, the DWBA does well. We illustrate this in Figure 3a. The physics underlying the form of the TDCS are easily understood in terms of a simple model [26] in which the target electron is assumed to be at rest relative to its nucleus, and the ionization process is viewed as a free collision between the incident and target electron. Two mechanisms leading to a coplanar symmetric final state may be distinguished. In the first, the incident electron collides with a target electron; conservation of energy and momentum would suggest that the electrons would emerge at 90° to each other. Of course, this is an over simplification since we should also take into account the fact that the target electron is not free but is in an atom with a definite binding energy and momentum distribution. Nevertheless, we would expect this mechanism to be responsible for the main peak near $\eta = 45^\circ$. The second mechanism involves a double collision in which the incident electron is first elastically backscattered from the nucleus, and then the ionization process is, as before, a nearly free electron–electron collision with the electrons emerging at right angles to each other but now in the backward directions, i.e., at $\eta = 135^\circ$. The DWBA contains both mechanisms, and we do as expected see two peaks at approximately the correct angles. It is instructive to perform a model calculation where the incident electron is replaced with a plane wave, and we designate this approximation as DWDWPW. Intuitively, in DWDWPW, the second mechanism is effectively "switched off". In Figure 3b, we show a comparison between the DWBA and the DWDWPW. As expected, the large angle peak has disappeared. In addition, in Figure 3b, we show the DWBA calculation for positron impact ionization. There is no large peak in the positron case but

rather an intimation of a suppressed structure where the peak should be. We interpret this as a reflection of the weaker backward scattering of positrons as compared to electrons.

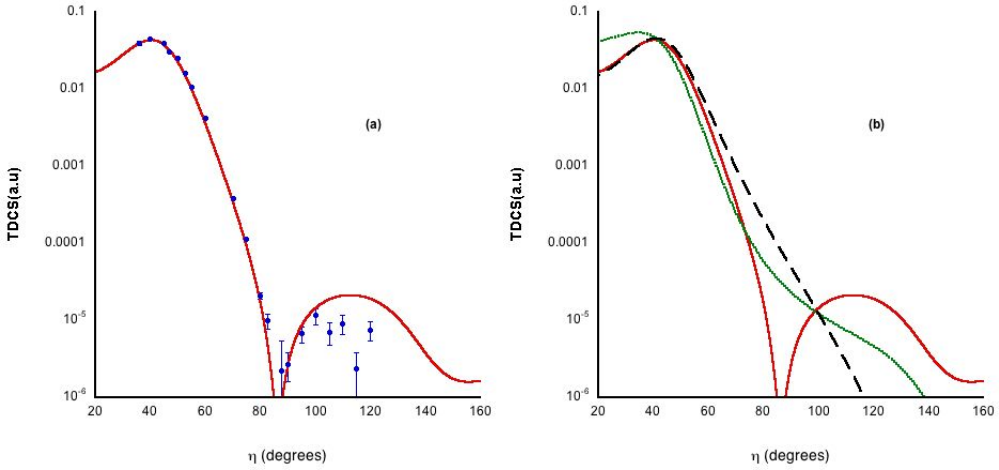

Figure 3. TDCS for the ionization of helium in coplanar symmetric geometry (i.e., $\Phi = 0°$) for $E_0 = 200$ eV. (**a**) Electron impact: experiment [25], theory DWBA (singlet exchange potential), no polarization no pci, experiment was relative and has been normalized to give the best visual fit to the DWBA; (**b**) Comparison of the TDCS calculated in the DWBA for positron: dotted green line, for electron: DWBA, solid red and the model calculation, DWDWPW, dashed black.

As the impact energy is lowered, the DWBA, as given by (1) and (2), performs less well. Experiment [24,27] finds a large angle peak that grows relative to the binary as the impact energy is decreased until it is approximately equal to the binary for $E_0 = 50$ eV [24]. On the other hand, the large angle peak in the DWBA remains orders of magnitude smaller. The DWBA takes no account of polarization or capture of the incoming electron into the final ion state, nor of electron–electron repulsion in the final state—all of which could be quite important not only as effects in themselves but also as they interfere with each other. In [12], an attempt was made to take these effects in a simple model: pci was included via the Gamov factor and an "ad-hock" polarization potential added in the initial and final channel, i.e.,

$$V_{pol} = \begin{cases} -\frac{\alpha}{2r^4} & r \geq r_0 \\ -\frac{\alpha}{2r_0{}^4} & r < r_0 \end{cases} \tag{12}$$

where $\alpha = 1.39$ was the polarizability of neutral helium $He(1s^2)$ in the incident channel and the polarizability of $He^+(1s)(\alpha = 0.28125)$ for the outgoing channels and $r_0 = 0.7565$. It was only with the combination of both pci and polarization for which shape agreement could be found with experiment. The polarization potential used in [12] was essentially chosen to give good agreement with the experiments of [24], but it worked well for a range of low energies. We show an example in Figure 4. Whelan et al. [28] extended the model to hydrogen where the incident channel polarization potential defined by analogy to He, i.e., α was taken to be the polarizability of H and

$$r_0^H = r_0^{He} \frac{< r >_H}{< r >_{He}} \tag{13}$$

where $< r >$ denotes the expectation value of r in the ground state of the atom. Whelan et al. [28] predicted that a double peak structure would be seen in coplanar symmetric geometry for H at an impact energy of 20 eV, a prediction that was immediately confirmed by experiment [29,30]. The positron results in Figure 4c show nothing of the structure found in the electron case.

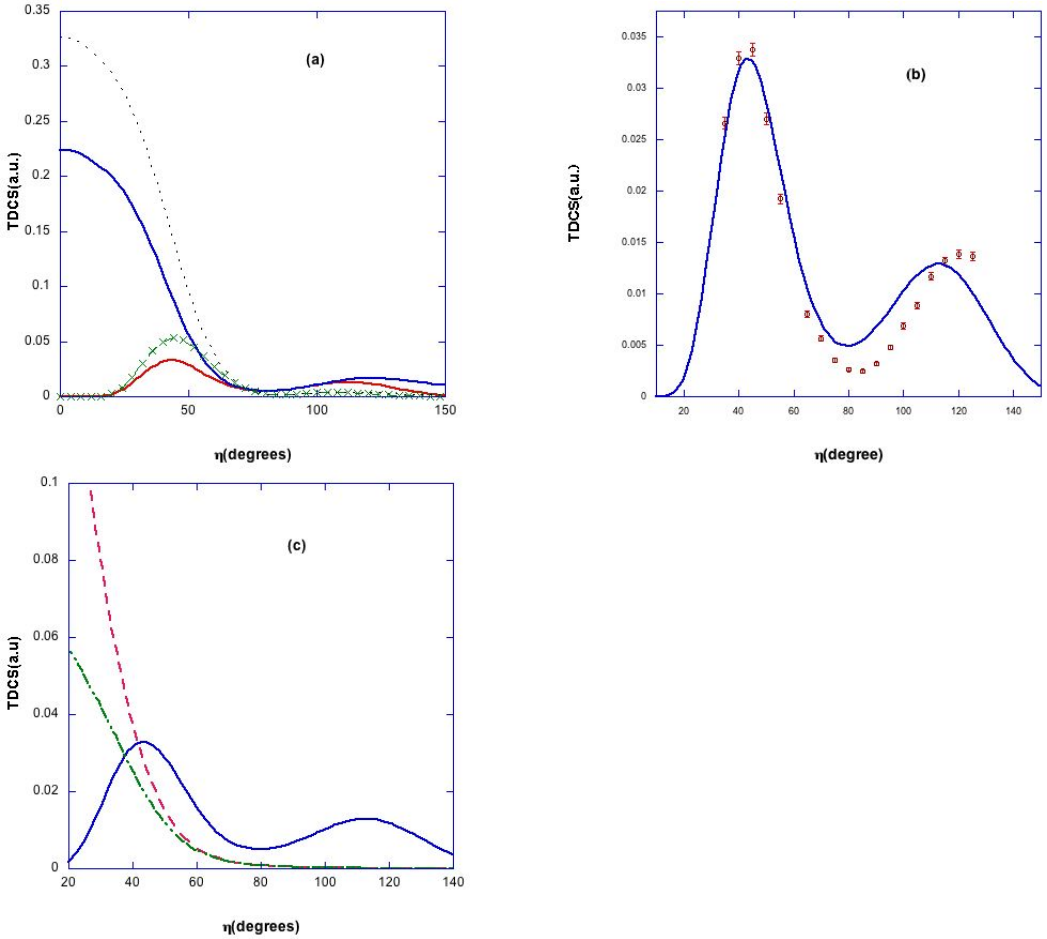

Figure 4. TDCS for the ionization of helium in coplanar symmetric geometry (i.e., $\Phi = 0°$) for $E_0 = 54.6$ eV. (**a**) Various theoretical curves for electron impact, dotted black: DWBA (singlet exchange potential); solid blue: DWBA (singlet exchange potential) with polarization but no pci, green dashed line with crosses: DWBA (singlet exchange potential) with pci but no polarization; red solid line, DWBA with polarization and pci; (**b**) Electron impact; experiment [27], theory DWBA (singlet exchange potential) with polarization and pci; (**c**) Solid blue curve DWBA (singlet exchange potential) for electron impact with polarization and pci, dashed red curve DWBA for positron impact with polarization and pci, green dashed-double dotted DWBA for positron impact with polarization but no pci.

3.2. Non Coplanar Energy Sharing Geometries

In the electron experiments of [31] on helium, the angle Φ was varied and a deep minimum in the TDCS observed for $\Phi = 67.5°$ (see Figure 5). In [20,32], DWBA calculations were presented, and the deep minimum reproduced. In the same paper, it was shown that the minimum existed even in the simplest calculation of this type where neither polarization nor post collisional electron–electron interaction was included. Rasch et al. explored the possibility of such distinct interference effects being observed in other targets, and they found that such a structure would be observed in other closed shell atoms but only for s states. They **predicted** such that it would be evident in $Ne(2s)$ at an impact energy of 110.5 eV for $\Phi \approx 42°$. This predication was subsequently confirmed [33]; see Figure 6. In addition, shown in this figure is the DWBA with $N_{e^-e^-}$ and the deep minimum is still visible, but, as would be expected, the cross section is reduced for smaller values of Θ_{12}. The equivalent positron impact calculation is also shown. The deep minimum has been replaced by a shallower and wider one, and the minimum value shifted towards smaller η values. The inclusion of $N_{e^+e^-}$ enhances the cross section for smaller Θ_{12} values.

In Figure 5, we show the experimental TDCS for the electron impact ionization of He [31] compared with our DWBA calculation, with and without pci. The minimum persists if shifted by a few degrees once polarization is added. Recently, in [34], this geometry was reexamined in a number of approximations. Their time dependent close coupling calculation (TDCC) is reasonably close to the DWBA, but their 3DW approximation only gives a shallow indentation at the critical angle, and, while both the Coulomb Born calculations (with and without $M_{e^-e^-}$) produce a deep minimum it has been shifted to larger angles away from the experiment and is four orders of magnitude too deep. In Figure 5b, we show the positron impact TDCS, in the DWBA, for the same kinematics. A deep minimum is no longer seen.

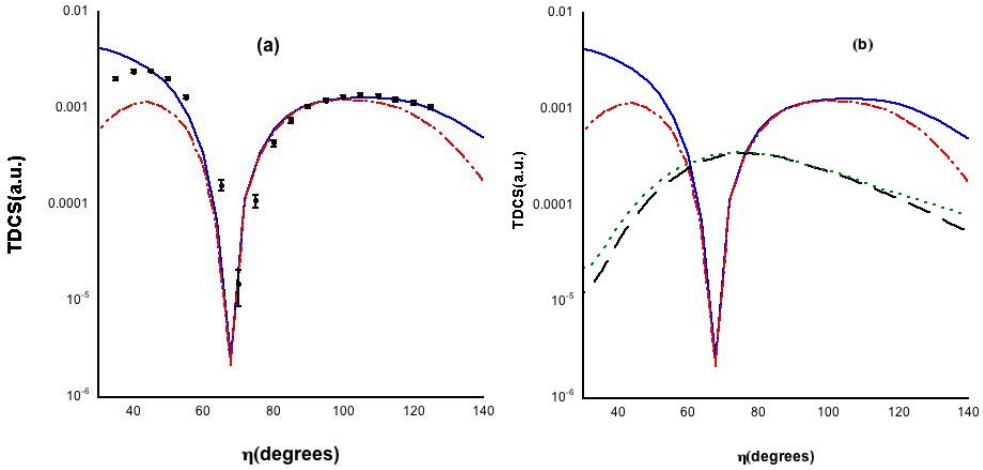

Figure 5. TDCS for ionization of helium with a projectile impact energy of $E_0 = 64.6$ eV, and "gun angle" of $\Phi = 67.5°$: (**a**) comparison of theory and experiment for electron impact, experiment [31]: solid blue curve DWBA (using singlet exchange) with no pci; red dashed double dotted DWBA (singlet exchange potential) with pci; (**b**) electron impact as in subfigure (**a**), positron impact black dashed DWBA (singlet exchange potential), no pci, dotted green, DWBA (singlet exchange potential) with pci.

In order to produce the sharp features seen in Figure 5, we undertook a series of model calculations, shown in Figure 7.

First, we considered a first Born approximation type calculation, i.e., a non exchange calculation with a plane wave for the incoming and scattered electron and the wavefunction of the ejected electron calculated in the static potential of the ion and no pci. Next, we added the $N_{e^-e^-}$ factor "switched on" the singlet static exchange potential distortion for the scattered electron; this we designate as PWDWPW. Then, we "switched on" distortion for the ejected electron, and this is our DWDWPW model. Finally, we replaced the scattered electron plane wave with a distorted wave to give us the regular DWBA. It is only when we have distorted waves in both the incident and final channels do we see the sharp minimum. The minimum is to be seen with and without pci and the inclusion of polarization makes no difference. It is found only when we include distortion for all the electrons. It is entirely absent from the positron calculation. Our model calculations indicate that it is not a result of pci nor of target polarization and is only present when we allow for the elastic scattering for both the incoming and outgoing electrons. The evaluation of the TDCS involves computing a six-dimensional integral over a highly oscillatory argument, and, as such, destructive interference effects may yield very small values for certain cases. This is the only explanation that is consistent with all the model calculations. Thus, we can interpret the structure as the result of a purely quantum mechanical interference effect. This is in agreement with the predictions of [20] for neon.

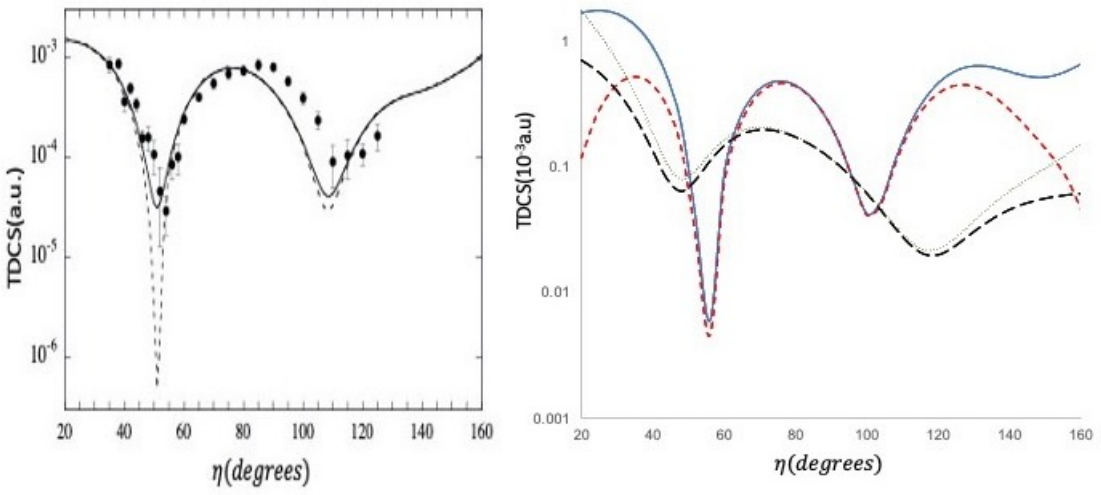

Figure 6. Left panel: TDCS for the electron impact ionization of $Ne(2s)$, $E_0 = 110.5$ eV, $\Phi = 42°$, experimental points [33]; solid line DWBA calculation of [20], dashed line theory convoluted over the experimental angular uncertainty. **Right panel**: TDCS for the electron and positron impact ionization of $Ne(2s)$, E = 37 eV, $\Phi = 40°$, electron impact DWBA (singlet exchange potential), solid blue, DWBA (singlet exchange potential)+$N_{e^-e^-}$ short dashed red, positron impact: DWBA, long dashed black, DWBA+$N_{e^+e^-}$, green dotted.

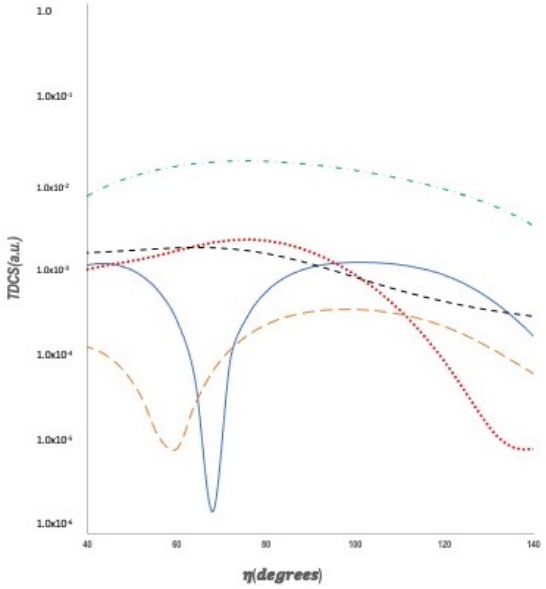

Figure 7. TDCS for the electron impact ionization of helium, $E_0 = 64.6$ eV, $\Phi = 67.5°$ comparison of different model calculations: 1st Born, as described in the text dotted black line; PWDWPW: purple dashed line; DWDWPW green dashed dotted line; DWBA solid blue line.

It is of interest to see if the same type of structure can be observed in open shell systems. In [13], a similar deep minimum was observed in the TDCS for the electron impact of hydrogen in coplanar symmetric geometry for an impact energy of 29 eV in a pure DWBA calculation with no pci or polarization. However, when pci and polarization are added, this deep minimum disappears, and this is probably a refection of the very strong polarization potential used. A recent paper [35] predicts, using a Coulomb Born (CB1) approximation, that there will be a deep minimum in the TDCS forthe positron impact ionization of hydrogen at an impact energy of 100 eV and a gun angle of 56.13°. We have repeated their calculation using the DWBA, (see Figure 8) and while there is something of the same feature in our DWBA calculations, our dip is seven orders of

magnitude shallower, and it is wider. This not altogether surprising since interference effects are very delicate, and it is likely that the position and magnitude of this effect in the Coulomb Born calculations of [35] will depend on their choice of effective charge, which is somewhat arbitrary.

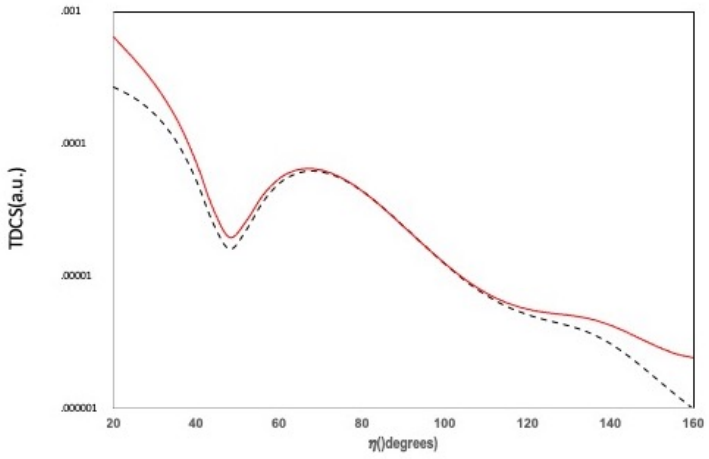

Figure 8. TDCS for the positron impact ionization of hydrogen in energy sharing geometry, $E_0 = 100$ eV, $\Phi = 56.13°$. DWBA:solid red DWBA $+N_{e^+e^-}$: dashed black

3.3. Energy Sharing Perpendicular Plane Geometry

There are experiments in the perpendicular plane [27,36], i.e., $\Phi = 90°$. These experiments were analyzed in [12,19] with a simple multiple scattering argument to explain the general behavior of the cross section and obtained very good agreement with the experiment using a DWBA approach. Within the DWBA, there are only two paths to the perpendicular plane:

1. Single scattering: For a free collision between an incident and a stationary electron resulting in two outgoing electrons of equal energy, conservation of energy and momentum requires all three vectors $\mathbf{k_0}, \mathbf{k_1}, \mathbf{k_2}$ to lie in the same plane with $\Theta_{12} = 90°$. Now, the atomic electron is not free but rather in a bound state with a momentum distribution, for both electrons to end up in the perpendicular plane as the result of a single collision, the incoming electron would have to collide with a bound electron that had momentum
$$\mathbf{k} = \boldsymbol{\kappa} - \mathbf{k}_0 \tag{14}$$
where $\boldsymbol{\kappa}.\mathbf{k}_0 = 0$, thus both electrons will emerge in the perpendicular plane with momentum $\boldsymbol{\kappa} = \mathbf{k_1} + \mathbf{k_2}$. Since the electron distribution in the helium atom is sharply peaked to zero, the most probable value will be
$$\begin{aligned} \boldsymbol{\kappa} &= \mathbf{0} \\ &= \mathbf{k_1} + \mathbf{k_2} \\ \Rightarrow \mathbf{k_1} &= -\mathbf{k_2} \\ \Rightarrow \Theta_{12} &= 180° \end{aligned} \tag{15}$$
Thus, for single scattering, one would expect a single peak at $\eta = 90°$. This is purely a wavefunction effect, and it would be misleading to interpret the back to back emission as being in some way related to the Wannier mechanism [37], since the peak is seen in the DWBA without pci.
2. Double scattering: here, the incoming electron is first elastically scattered into the plane perpendicular to the incoming beam and then in a second collision ionizes the atom with both final state electrons coming out at roughly 90° to each other.

As $\|\mathbf{k}_0\|$ increases, it becomes more difficult for the electron to ionize via the single scattering mechanism and thus the double scattering mechanism will dominate at higher energies, and the most favorable condition for single scattering will be $\mathbf{k}_0 \approx \mathbf{0}$. This interpretation was is in qualitative accordance with the experiment of [27,36]. At the lowest energy, a single peak at $\eta = \frac{\Theta_{12}}{2} = 90^\circ$ is observed. As the impact energy is increased, secondary peaks are observed in the vicinity of $\eta = 45^\circ$ and 135°.

The DWBA calculations [12] reproduce these features and are generally in good agreement with the relative experiments. At low energies, Ehrhardt and collaborators [38,39] measured the cross sections for a fixed angle of $\Theta_{12} = 180^\circ$, and a common point to all the planes was obtained by rotating the gun angle. In Figure 9 (left panel), we show a comparison between this absolute measurement and the distorted wave approximation scaled by the $M_{e^-e^-}$ and $N_{e^-e^-}$, with the latter normalized to 1 when $\Theta_{12} = 180^\circ$. The DWBA $+N_{e^-e^-}$ is in remarkably good agreement with the absolute experimental value while the DWBA+$M_{e^-e^-}$ is significantly too small. The DWBA with $N_{e^-e^-}$ also gives a better fit to the relative measurements of [40] (middle panel). In Figure 9 (right panel), we also show a comparison between the $(e^-, 2e^-)$ and (e^+, e^+e^-) cross sections, for the small energy E values. In both the electron and positron cases, there is no indication of a double scattering peak, and the positron cross section is much smaller.

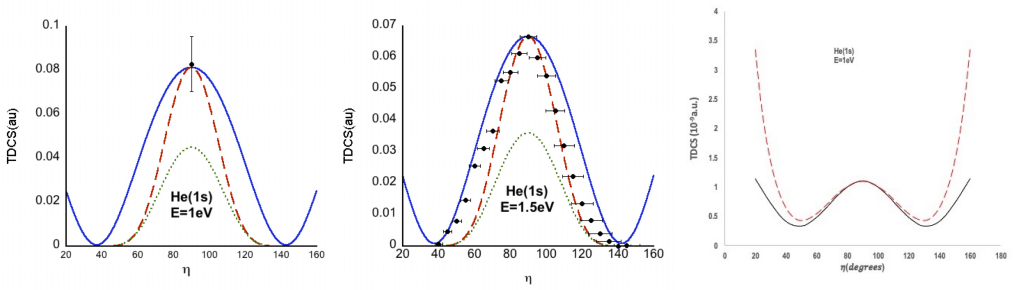

Figure 9. TDCS for the ionization of helium with $\Phi = 90^\circ, \theta_1 = \theta_2 = \eta, E_1 = E_2 = E$ eV. Electron impact: The absolute measurement of [38] (**left panel**) is shown, and the relative measurements of [40] (**middle panel**) the DWBA (triplet exchange) without pci, solid blue line; DWBA with $N_{e^-e^-}$ factor normalized to 1 at $\Theta = 180^\circ$, dashed red line, DWBA with $M_{e^-e^-}$ dotted green line; Positron impact (**right panel**): DWBA without pci, solid black line, DWBA $+N_{e^+e^-}$, dashed red.

In Figure 10, we show a comparison between theory and experiment for $E_0 = 64.6$, $E = 20$ eV. The "double scattering" peaks are visible in the electron case for DWBA without pci, and its addition tends to suppress the peaks at 45° and 135°, even though they are still clearly visible in the measurement. It would appear that, in this case, the use of N_{e-e-} is too strong. We also show the DWBA for positron impact which is now almost structureless and much smaller in size.

In the positron case, the cross section is greatly reduced in absolute size, and the double scattering peaks at $\eta \approx 45^\circ$ and $\eta \approx 13^\circ$ are missing for all impact energies. For our lowest energy $E_1 = E_2 = 1$ eV, in Figure 9, we do see a peak in the positron case for $\eta = 90^\circ$, but the maximum value is much smaller than in the electron case. For $E_1 = E_2 = 20$ eV, this peak completely disappears.

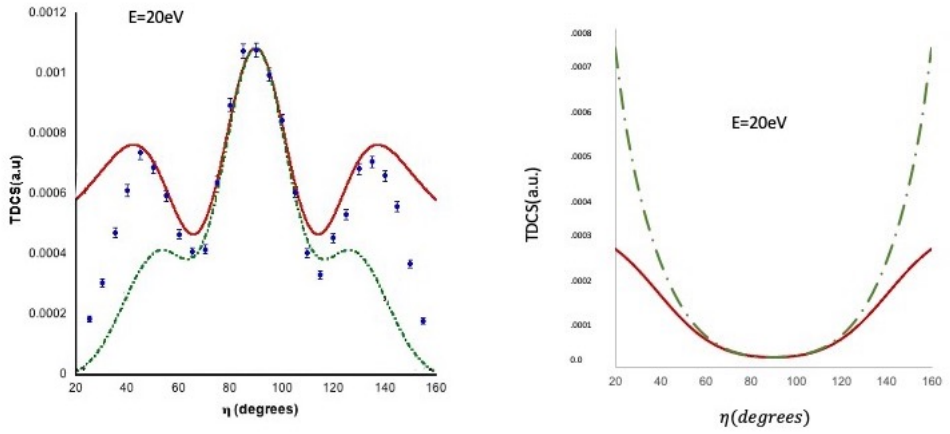

Figure 10. TDCS for electron (**left panel**) and positron impact (**right panel**) ionization of helium in the perpendicular plane ($\Phi = 90°$), $E_0 = 64.6$ eV, experimental points [31]. The theoretical curves are: solid red curve: DWBA with no pci; green dashed dotted DWBA with pci.

4. Conclusions

Our electron scattering calculations show many interesting structures that highlight different and sometimes competing few body effects. In coplanar symmetric geometry, we find that, for high impact energies, the DWBA theory correctly reproduces the experimental results. However, for low impact energies, the agreement with the experiment is obtained only by adding corrections for both polarization and post-collisional electron–electron interaction. For non-coplanar symmetric geometries, a deep minimum in the TDCS is seen experimentally for certain gun angles. The DWBA theory reproduces this minimum even without polarization and pci. We interpret these structures in terms of interference effects, and it is necessary to allow for both the elastic scattering of the incoming electron and the exiting electrons if these structures are to appear. The experimental data in the perpendicular plane are well reproduced by the DWBA approximation that allows for two different pathways into the perpendicular plane, a single scattering mechanism at low impact energies, and a multiple scattering mechanism at elevated energies. The equivalent structures in the positron case are much less pronounced. Indeed, we find little evidence for the strong interference effects that are seen in the TDCS for e^+ on atomic hydrogen in the Coulomb Born calculations of [35]. The particular structures predicted in the Coulomb Born calculations are probably an artifact of the choice of effective charge.

Author Contributions: Both authors worked closely together during the entire project including the writing of this paper. All authors have read and agreed to the published version of the manuscript.

Funding: The research received financial support from the Natural Science and Engineering Research Council of Canada.

Acknowledgments: We thank Andrew Murray for supplying us with his data.

Conflicts of Interest: The authors declare no conflict of interest.

References

1. Du Bois, R.D.; Gavin, J.; de Lucio, O.G. Differential cross sections for ionization of argon by 1 keV positron and electron impact. *J. Phys. Conf. Ser.* **2014**, *488*, 072004. [CrossRef]
2. Gavin, J.; de Lucio, O.G.; DuBois, R.D. Triply differential measurements of single ionization of argon by 1-keV positron and electron impact. *Phys. Rev. A* **2017**, *95*, 062703. [CrossRef]
3. Campeanu, R.I.; Walters, H.R.J.; Whelan, C.T. The electron and positron impact ionization of inert gases. *Phys. Rev. A* **2018**, *97*, 062702. [CrossRef]
4. Miller, F.K.; Whelan, C.T.; Walters, H.R.J. Energy sharing (e,2e) collisions-ionization of the inert gases in the perpendicular plane. *Phys. Rev. A* **2015**, *91*, 012706. [CrossRef]

5. Curran, E.P.; Whelan, C.T.; Walters, H.R.J. On the electron impact ionisation of H(1s) in coplanar asymmetric geometry. *J. Phys. B At. Mol. Opt. Phys.* **1991**, *24*, L19. [CrossRef]
6. Lucey, S.P.; Rasch, J.; Whelan, C.T. On the use of analytic ansatz wavefunctions in the study of (e,2e) processes. *Proc. R. Soc. A* **1999**, *455*, 349. [CrossRef]
7. Rasch, J.; Whelan, C.T.; Allan, R.J.; Walters, H.R.J. The normalization of the experimental triple differential cross section of noble gas atoms in extreme asymmetric geometry. In *Electron and Photon Impact Ionization*; Whelan, C.T., Walters, H.R.J., Eds.; Plenum: New York, NY, USA, 1997; pp. 305–318.
8. Walters, H.R.J. Perturbative methods in electron- and positron-atom scattering. *Phys. Rep.* **1984**, *116*, 1. [CrossRef]
9. Curran, E.P.; Walters, H.R.J. Triple differential cross sections for electron impact ionisation of atomic hydrogen—A coupled pseudostate calculation. *J. Phys. B At. Mol. Opt. Phys.* **1987**, *20*, 333. [CrossRef]
10. Bartlett, P.L.; Stelbovics, A.T. The application of propagating exterior complex scaling in atomic collisions. In *Fragmentation Processes: Topics in Atomic and Molecular Physics*; Whelan, C.T., Ed.; Cambridge University Press: Cambridge, UK, 2013; pp. 48–71.
11. Madision, D.H.; Calhoun, R.V.; Shelton, W.N. Triple-differential cross sections for electron-impact ionization of helium. *Phys. Rev. A* **1977**, *16*, 552. [CrossRef]
12. Whelan, C.T.; Allan, R.J.; Walters, H.R.J.; Zhang, X. (e,2e), effective charges, distorted waves and all that ! In $(e, 2e)$ & *Related Processes*; Whelan, C.T., Walters, H.R.J., Lahmam-Bennani, A., Ehrhardt, H., Eds.; Kluwer: Dordrecht, The Netherlands, 1993; pp. 33–74.
13. Rasch, J. (e,2e) Processes with Neutral Atom Targets. Ph.D. Thesis, University of Cambridge, Cambridge, UK, 1996.
14. Clementi, E.; Roetti, C. Roothan-Hartree-Fock atomic wavefunctions. *At. Data Nucl. Data Tables* **1974**, *14*, 177. [CrossRef]
15. Furness, J.B.; Carthy, I.E.M. Semi phenomenological optical model for electron scattering. *J. Phys. B At. Mol. Opt. Phys.* **1973**, *6*, 2280. [CrossRef]
16. Riley, M.E.; Truhlar, D.G. Approximations for exchange potentials in electron scattering. *J. Chem. Phys.* **1975**, *63*, 2182. [CrossRef]
17. Martinez, J.M.; Walters, H.R.J.; Whelan, C.T. The electron impact ionization of one and two electron atoms and ions close to the ionization threshold. *J. Phys. B At. Mol. Opt. Phys.* **2008**, *41*, 065202. [CrossRef]
18. Bransden, B.H.; McDowell, M.R.C.; Noble, C.J.; Scott, T. Equivalent exchange potentials in electron scattering. *J. Phys. B At. Mol. Opt. Phys.* **1976**, *9*, 1301. [CrossRef]
19. Zhang, X.; Whelan, C.T.; Walters, H.R.J. (e,2e) cross sections for the ionisation of helium in coplanar symmetric geometry. *J. Phys. B At. Mol. Opt. Phys.* **1990**, *23*, L509. [CrossRef]
20. Rasch, J.; Whelan, C.T., Allan, R.J.; Lucey, S.P.; Walters, H.R.J. Strong interference effects in the triple differential cross section of neutral atom targets. *Phys. Rev. A* **1997**, *56*, 1379. [CrossRef]
21. Botero, J.; Macek, J.H. Threshold angular distributions of(e,2e) cross sections of helium atoms. *Phys. Rev. Lett.* **1992**, *68*, 576. [CrossRef]
22. Ward, S.J.; Macek, J.H. Wave functions for continuum states of charged fragments. *Phys. Rev. A* **1994**, *49*, 1049. [CrossRef]
23. Pochat, A.; Tweed, R.J.; Peresses, J.; Joachain, J.; Piraux, C.B.; Byron, F.W., Jr. Second-order effects in large-angle coplanar symmetric (e, 2e) processes. *J. Phys. B At. Mol. Opt. Phys.* **1983**, *16*, L755. [CrossRef]
24. Rösel, T.; Dupré, C.; Röder, J.; Duguet, A.; Jung, K.; Lahmam-Bennani, A.; Ehrhardt, H. Coplanar symmetric(e,2e) cross sections on helium and neon. *J. Phys. B At. Mol. Opt. Phys.* **1991**, *24*, 3059. [CrossRef]
25. Frost, L.; Freienstein, P.; Wagner, M. 200 eV coplanar symmetric (e,2e) on helium: A sensitive test of reaction models. *J. Phys. B At. Mol. Opt. Phys.* **1990**, *23*, L715. [CrossRef]
26. Zhang, X.; Whelan, C.T.; Walters, H.R.J. Energy sharing (e,2e) collisions-ionisation of Helium in the perpendicular plane. *J. Phys. B At. Mol. Opt. Phys.* **1990**, *23*, L173. [CrossRef]
27. Murray, A.J. Electron impact ionization using (e,2e) coincidence techniques from threshold to intermediate energies. In *Fragmentation Processes: Topics in Atomic and Molecular Physics*; Whelan, C.T., Ed.; Cambridge University Press: Cambridge, UK, 2013; pp. 164–206.
28. Whelan, C.T.; Allan, R.J.; Walters, H.R.J. PCI, polarisation and exchange effects in (e,2e) collisions *J. Phys. IV* **1993**, *3*, C6. [CrossRef]
29. Röder, J.; Rasch, J.; Jung, K.; Whelan, C.T.; Ehrhardt, H.; Allan, J.R.; Walters, H.R.J. Coulomb 3 body effects in low energy electron impact ionization of H(1s). *Phys. Rev. A* **1994**, *53*, 225. [CrossRef]
30. Whelan, C.T.; Allan, R.J.; Rasch, J.; Walters, H.R.J.; Zhang X.; Röder, J.; Jung, K.; Walters, H.R.J.; Ehrhardt, H. Coulomb 3-body effects in (e,2e) Collisions: The ionisation of H in coplanar symmetric geometry. *Phys. Rev. A* **1994**, *50*, 4394. [CrossRef]
31. Murray, A.J. Electron impact ionization using (e,2e) coincidence techniques from threshold to intermediate energies. In $(e, 2e)$ & *Related Processes*; Whelan, C.T., Walters, H.R.J., Lahmam-Bennani, A., Ehrhardt, H., Eds.; Kluwer: Dordrecht, The Netherlands, 1993; pp. 327–340.
32. Rasch, J.; Whelan, C.T.; Allan, R.J.; Walters, H.R.J. An explanation of the structure observed in out of plane symmetric measurements on helium. In *Electron and Photon Impact Ionization*; Whelan, C.T., Walters, H.R.J., Eds.; Plenum: New York, NY, USA, 1997; pp. 185–193.
33. Murray, A.J.; Read, F.H. Deep interference minima in experimental ionization differential cross sections. *Phys. Rev. A* **2000**, *63*, 012714. [CrossRef]

34. DeMars, C.M.; Kent, J.B.; Ward, S.J. Deep minima in the Coulomb-Born triply differential cross sections for ionization of helium by electron and positron impact. *Eur. Phys. J. D* **2020**, *74*, 48. [CrossRef]
35. DeMars, C.M.; Ward, S.J.; Colgan, J.; Amari, S.; Madison, D.H. Deep Minima in the Triply Differential Cross Section for Ionization of Atomic Hydrogen by Electron and Positron Impact. *Atoms* **2020**, *8*, 26. [CrossRef]
36. Woolf, M.B.J. (e,2e) Measurements in the Perpendicular Plane. Ph.D. Thesis, University of Manchester, Manchester, UK, 1996.
37. Wannier, G.H. The threshold law for single ionization of atoms or ions by electrons. *Phys. Rev.* **1953**, *90*, 817. [CrossRef]
38. Ehrhardt, H.; Rösel, T. Near threshold (e,2e) ionisation of helium and atomic hydrogen. In $(e, 2e)$ & *Related Processes*; Whelan, C.T., Walters, H.R.J., Lahmam-Bennani, A., Ehrhardt, H., Eds.; Kluwer: Dordrecht, The Netherlands, 1993; pp. 76–82.
39. Rösel, T.; Röder, J.; Frost, L.; Jung, K.; Ehrhardt, H.; Jones, S.; Madison, D.H. Absolute triple differential cross section for ionization of helium near threshold. *Phys. Rev. A* **1992**, *46*, 2539. [CrossRef] [PubMed]
40. Nixon, K.L.; Murray, A.J.; Kaiser, C. Low energy (e,2e) studies of the noble gases in the perpendicular plane. *J. Phys. B At. Mol. Opt. Phys.* **2010**, *43*, 085202. [CrossRef]